

Supplementary Materials for

Photochemical degradation affects the light absorption of water-soluble brown carbon in the South Asian outflow

Sanjeev Dasari, August Andersson, Srinivas Bikkina, Henry Holmstrand, Krishnakant Budhavant, Sreedharan Satheesh, Eija Asmi, Jutta Kesti, John Backman, Abdus Salam, Deewan Singh Bisht, Suresh Tiwari, Zahid Hameed, Örjan Gustafsson*

*Corresponding author. Email: orjan.gustafsson@aces.su.se

Published 30 January 2019, *Sci. Adv.* **5**, eaau8066 (2019)
DOI: 10.1126/sciadv.aau8066

This PDF file includes:

- Note S1. A theoretical model for ruling out marine-biogenic source contribution.
- Note S2. A theoretical model for the degradation of WSOC and WIOC in the South Asian outflow.
- Note S3. A conceptual aging model for the joint time and wavelength dependence of MAC_{WS-BrC} .
- Note S4. Absorption measurements of MAC_{WS-BrC} and AAE.
- Note S5. Estimating the imaginary part of the refractive index of WS-BrC.
- Note S6. Testing a putative effect of pH on WS-BrC optical properties over the South Asian region.
- Fig. S1. Air mass clusters during SAPOEX-16.
- Fig. S2. Fractional contribution of air mass clusters during SAPOEX-16.
- Fig. S3. Concentrations of EC, OC, and WSOC during SAPOEX-16.
- Fig. S4. Imaginary part of the refractive index (K_{WS-BrC}) at 365 nm.
- Fig. S5. Asserting the peripheral contribution of marine-biogenic sources at MCOH during SAPOEX-16.
- Fig. S6. Testing a putative effect of pH on WS-BrC optical properties.
- Fig. S7. Constraining the mixing of WSOC sources on WS-BrC light absorption in the South Asian outflow.
- Fig. S8. Degradation of WSOC and WIOC during long-range transport in the South Asian outflow.
- Table S1. Concentrations (mean \pm SD) and element mass ratios of carbonaceous species during SAPOEX-16.
- Table S2. pH of aerosol WSOC extracts during SAPOEX-16.

Note S1. A theoretical model for ruling out marine-biogenic source contribution.

We consider that the mass-absorption cross section (MAC_{WS-BrC}) for light-absorbing water-soluble organic carbon (WSOC) is composed of a mixture of terrestrial (terr) and marine (mar) contributions

$$MAC_{WS-BrC} = \frac{b_{abs}}{WSOC} = \frac{b_{terr} + b_{mar}}{WSOC_{terr} + WSOC_{mar}} \approx \frac{b_{terr}}{WSOC_{terr} + WSOC_{mar}} \quad (1)$$

The marine WSOC absorption is substantially low ($b_{mar} \approx 0$).

Defining the fraction terrestrial (f) as:

$$f = \frac{WSOC_{terr}}{WSOC_{terr} + WSOC_{mar}} \quad (2)$$

Combining Eqs (1) and (2):

$$MAC_{WS-BrC} = \frac{b_{terr} \cdot f}{WSOC_{terr}} \quad (3)$$

Assuming isotopic mass-balance we have (obs = observed)

$$\delta^{13}C_{obs} = f \cdot \delta^{13}C_{terr} + (1 - f) \cdot \delta^{13}C_{mar} \quad (4)$$

Thus

$$f = \frac{\delta^{13}C_{obs} - \delta^{13}C_{mar}}{\delta^{13}C_{terr} - \delta^{13}C_{mar}} \quad (5)$$

Combining Eqs (3) and (5)

$$MAC_{WS-BrC} = \frac{b_{terr}}{WSOC_{terr}} \cdot \left(\frac{\delta^{13}C_{obs} - \delta^{13}C_{mar}}{\delta^{13}C_{terr} - \delta^{13}C_{mar}} \right) \quad (6)$$

Noting that the $\delta^{13}C$ terrestrial and marine endmembers are constants, we can for clarity reformulate Eq (6) as (k_1 and k_2 constants)

$$MAC_{WS-BrC} = \frac{b_{terr}}{WSOC_{terr}} \cdot (k_1 \cdot \delta^{13}C_{obs} + k_2) \quad (7)$$

Based on Eq.7, if the mixing of terrestrial and marine sources drives the changes of MAC_{WS-BrC} and $\delta^{13}C$ for different sites, a linear-relation between MAC_{WS-BrC} and $\delta^{13}C$ is expected. However, $\log(MAC_{WS-BrC})$ vs $\log(\delta^{13}C)$ gives a better fit (see fig. S7) and we thus conclude that mixing of terrestrial and marine sources is not the cause of the observed effects on light-absorption of BrC during SAPOEX-16. The dependence of MAC_{WS-BrC} and $\delta^{13}C$ is derived in Note S3.

Note S2. A theoretical model for the degradation of WSOC and WIOC in the South Asian outflow.

The organic carbon pool can be divided into water-soluble and water-insoluble fractions. A theoretical-model is presented to elucidate the effects of atmospheric processing during transport on these fractions of organic carbon. A basic assumption implicit to this model is that both water-soluble organic carbon (WSOC) and water-insoluble organic carbon (WIOC) are degrading between source-to-receptor sites as well as a fraction of WIOC is oxidized to WSOC during long-range transport. Other assumptions included in the model are that there are no substantial additional emissions during over-ocean transport contributing to WSOC. All assumptions are for the net WSOC and WIOC pool.

We begin the model by formulating the net averaged loss rates of WSOC and WIOC.

$$\frac{dWSOC}{dt} = -k_1 \cdot WSOC + k_2 \cdot WIOC \quad (8)$$

$$\frac{dWIOC}{dt} = -(k_2 + k_3) \cdot WIOC \quad (9)$$

Where k_1 and k_3 are the rate of degradation of WSOC and WIOC respectively. k_2 is the rate of oxidation/conversion of WIOC to WSOC during transport

Solving Eq.9 :

$$WIOC = WIOC_0 \cdot e^{-(k_2+k_3) \cdot t} \quad (10)$$

Incorporating Eq.10 in Eq.8 we get

$$WSOC = \left(WSOC_0 - \frac{k_2 \cdot WIOC_0}{k_1 - (k_2 + k_3)} \right) \cdot e^{-k_1 \cdot t} + \frac{k_2 \cdot WIOC_0}{k_1 - (k_2 + k_3)} \cdot e^{-(k_2 + k_3) \cdot t} \quad (11)$$

We then use the simple expression of WSOC/OC as a combination of WIOC and WSOC

$$\frac{WSOC}{OC} = \frac{WSOC}{WSOC+WIOC} \quad (12)$$

Setting $k = (k_2 + k_3) - k_1$, and noting that $k > 0$

$$\frac{WSOC}{OC} = \frac{\left(WSOC_0 + \frac{k_2 \cdot WIOC_0}{k}\right) - \frac{k_2 \cdot WIOC_0}{k} \cdot e^{-k \cdot t}}{\left(WSOC_0 + \frac{k_2 \cdot WIOC_0}{k}\right) + WIOC_0 \cdot \left(1 - \frac{k_2 \cdot WIOC_0}{k}\right) \cdot e^{-k \cdot t}} \quad (13)$$

Defining constants A and B , we can write this in the form

$$\frac{WSOC}{OC} = \frac{1+A \cdot e^{-k \cdot t}}{1+B \cdot e^{-k \cdot t}} \quad (14)$$

Using Eq.24 from Note. S3 and substituting in Eq.14

We then arrive at a fitting function of the form

$$\frac{WSOC}{OC} = \frac{1+A \cdot \left(\frac{\delta^{13}C}{1000} + 1\right)^k}{1+B \cdot \left(\frac{\delta^{13}C}{1000} + 1\right)^k} \quad (15)$$

Eq.15 suggests that transfer between two OC pools (WIOC to WSOC) in addition to oxidative transformation during long-range transport as possible factors governing the enrichment of the mass fraction of WSOC in the South Asian outflow (shown in fig. S8).

Note S3. A conceptual aging model for the joint time and wavelength dependence of MAC_{WS-BrC} .

The time evolution of water-soluble Brown Carbon (WS-BrC) in the atmosphere is inherently complex, including source variability, secondary formation, phase transitions, transfer between different OC pools (e.g., WSOC to WIOC), preferential deposition, the dynamics of the non-absorbing components of WSOC and the photo-chemical break-down (bleaching) of chromophores. Here, a conceptual aging model is presented based on the postulation that bleaching is the main driver of the time evolution of WS-BrC light-absorption and stable carbon isotope signature $\delta^{13}C_{WSOC}$, during long-range transport in the South Asian outflow.

The aging model is based on the assumption that during over-ocean transport in the South Asian outflow there are no substantial additional source emissions contributing to WSOC as well as no significant contribution to light-absorption from the secondary aerosol formation. Within this aging model, we establish inter-dependencies of WS-BrC optical parameters and the aging proxy ($\delta^{13}C$).

The model consists of the following three steps:

- a) Time evolution of stable carbon isotope signature of WSOC
- b) Time evolution of WS-BrC light-absorption parameter (MAC_{WS-BrC})
- c) Time evolution of WS-BrC light-absorption parameter (AAE)

a) *Time evolution of stable carbon isotope signature of WSOC*

Consider that the light-absorption (b_{abs}) of the light (^{12}C) and heavy (^{13}C) isotopes of water-soluble organic carbon (WSOC) degrade with first-order kinetics during atmospheric transport:

$$[b]_t = [b]_0 \cdot e^{-k_b \cdot t} \quad (16a)$$

$$[WSO^{12}C]_t = [WSO^{12}C]_0 \cdot e^{-k_{12} \cdot t} \quad (16b)$$

$$[WSO^{13}C]_t = [WSO^{13}C]_0 \cdot e^{-k_{13} \cdot t} \quad (16c)$$

Where $[WSOC]_t$ is the concentration at time t and $[WSOC]_0$ is the concentration at time 0, and k_b, k_{12}, k_{13} are the first-order rate constants for the parameters $b_{abs}, ^{12}C, ^{13}C$ respectively.

The stable carbon isotope signature is reported (in per mil) as

$$[\delta^{13}C] = ((13C/12C)_{sample} / (13C/12C)_{standard} - 1) \times 1000 \quad (17)$$

The time evolution of $\delta^{13}C_{WSOC}$ can be given as

$$[\delta^{13}C]_t = \left(\frac{[WSO^{13}C]_t}{[WSO^{12}C]_t} \right)_{sample} / \left(\frac{[WSO^{13}C]}{[WSO^{12}C]} \right)_{standard} - 1) \times 1000 \quad (18)$$

Writing $(WSO^{13}C / WSO^{12}C)_{standard}$ as STD (as this is always constant), we can reformulate Eq.(18) as

$$[\delta^{13}C]_t = \left(\frac{\left(\frac{[WSO^{13}C]}{[WSO^{12}C]} \right)_t^{sample}}{STD} - 1 \right) \times 1000 \quad (19)$$

Substituting the values from Eq. (16b) and (16c)

$$[\delta^{13}C]_t = \left(\frac{\left[\frac{[WSO^{13}C]_0 \cdot e^{-k_{13} \cdot t}}{[WSO^{12}C]_0 \cdot e^{-k_{12} \cdot t}} \right]_{sample}}{STD} - 1 \right) \times 1000 \quad (20)$$

$$[\delta^{13}C]_t = \left(\frac{[WSO^{13}C]_0 \cdot e^{-(k_{13}-k_{12}) \cdot t}}{WSO^{12}C(0) \cdot STD} - 1 \right) \times 1000 \quad (21)$$

$$\text{Defining: } Q \equiv \left(\frac{[\delta^{13}C]_t}{1000} + 1 \right) \cdot STD, \text{ we have:} \quad (22)$$

$$\frac{[WSO^{13}C]_0 \cdot e^{-(k_{13}-k_{12}) \cdot t}}{[WSO^{12}C]_0} = Q \quad (23)$$

Inverting Eq. (23)

$$t = -\frac{1}{(k_{13}-k_{12})} \ln \left| Q \cdot \frac{[WSO^{12}C]_0}{[WSO^{13}C]_0} \right| \quad (24)$$

Eq.24 establishes a dependency of transport-time and aging proxy $\delta^{13}C$

b) Time evolution of WS-BrC light-absorption parameter (MAC_{WS-BrC})

The time evolution of WS-BrC mass-absorption cross section (MAC_{WS-BrC}) is given as

$$(MAC_{WS-BrC})_t = \frac{[b]_t}{[WSOC]_t} = \frac{[b]_t}{[WSO^{12}C]_t + [WSO^{13}C]_t} = \frac{[b]_0 \cdot e^{-k_b \cdot t}}{[WSO^{12}C]_0 \cdot e^{-k_{12} \cdot t} + [WSO^{13}C]_0 \cdot e^{-k_{13} \cdot t}} \quad (25)$$

Combining Eq. (24) and (25)

$$MAC_{WS-BrC(Q)} = \frac{b_0 \cdot \left[Q \cdot \frac{WSO^{12}C_0}{WSO^{13}C_0} \right]^{k_b/(k_{13}-k_{12})}}{WSO^{12}C_0 \cdot \left[Q \cdot \frac{WSO^{12}C_0}{WSO^{13}C_0} \right]^{k_{12}/(k_{13}-k_{12})} + WSO^{13}C_0 \cdot \left[Q \cdot \frac{WSO^{12}C_0}{WSO^{13}C_0} \right]^{k_{13}/(k_{13}-k_{12})}} \quad (26)$$

which can be written as

$$MAC_{WS-BrC(Q)} = \frac{\frac{b_0}{WSO^{12}C_0} \cdot \left(Q \cdot \frac{WSO^{12}C_0}{WSO^{13}C_0} \right)^{(k_b-k_{12})/(k_{13}-k_{12})}}{1+Q} \quad (27)$$

We can summarize Eq. (27) with the following relation (C_1 and $C_2 = \text{constants}$)

$$MAC_{WS-BrC(Q)} = \frac{C_1 \cdot Q^{C_2}}{1+Q} \approx C_1 \cdot Q^{C_2} \quad (28)$$

We note that typically $Q \ll 1$, which justifies the approximation in Eq. (28).

Eq. (28) is a fitting routine for the inter-dependence between time evolution of WS-BrC light-absorption (MAC_{WS-BrC}) and $\delta^{13}C_{WSOC}$ *i.e.* aging due to atmospheric oxidation in the outflow from South Asia between source-to-receptor sites, parameterized by constants C_1 and C_2 .

c) Time evolution of WS-BrC light-absorption parameter (AAE)

The wavelength-dependence of the MAC_{WS-BrC} is typically given by:

$$MAC_{WS-BrC}(\lambda) = MAC_{WS-BrC}(\lambda_{ref}) \cdot \left(\frac{\lambda}{\lambda_{ref}}\right)^{-AAE} \quad (29)$$

Eq. (25) gives the time-dependence of the MAC_{WS-BrC} at a given wavelength.

Now we want to combine equations 25, 29 to explore the joint time and wavelength-dependence of the MAC_{WS-BrC} , emphasizing the wavelength-dependence of the degradation constant ($k_b(\lambda)$) and that $AAE(0)$ is the AAE at time $t = 0$

$$MAC_{WS-BrC}(t, \lambda) = \frac{b(0, \lambda_{ref}) \cdot e^{-k_b(\lambda) \cdot t}}{WSOC(0) \cdot e^{-k_{WSOC} \cdot t}} \cdot \left(\frac{\lambda}{\lambda_{ref}}\right)^{-AAE(0)} \quad (30)$$

For clarity, we do not consider the division of WSOC into the two stable carbon isotopes in this equation. From observations, we know that the wavelength-dependence follows a power law at all times, and thus:

$$\left(\frac{\lambda}{\lambda_{ref}}\right)^{-AAE(t)} \propto e^{-k(\lambda) \cdot t} \cdot \left(\frac{\lambda}{\lambda_{ref}}\right)^{-AAE(0)} \rightarrow e^{-k(\lambda) \cdot t} = e^{-k_{ref} \cdot t} \cdot \left(\frac{\lambda}{\lambda_{ref}}\right)^{-k_{AAE} \cdot t} \quad (31)$$

Where k_{AAE} is the wavelength-dependent rate constant and k_{ref} is the rate constant at the reference wavelength. Thus, the joint time- and wavelength-dependence of the MAC_{WS-BrC} may be written as:

$$MAC_{WS-BrC}(t, \lambda) = MAC_{WS-BrC}(0, \lambda_{ref}) \cdot e^{-(k_{ref}-k_{WSOC}) \cdot t} \cdot \left(\frac{\lambda}{\lambda_{ref}}\right)^{-(k_{AAE} \cdot t + AAE(0))} \quad (32)$$

The time-dependence of the AAE is thus given by

$$AAE(t) = k_{AAE} \cdot t + AAE(0) \quad (33)$$

Combining Eq. (24), (33), we have ($C_3, C_4 = \text{constants}$):

$$AAE(Q) = -C_3 \cdot \ln|C_4 \cdot Q| + AAE(0) \quad (34)$$

Data fitting routines

We can summarize the results with two data fitting routines for the inter-dependence between MAC_{WS-BrC} , AAE and $\delta^{13}C$, parametrized by constants C_1, C_2, C_3, C_4

$$MAC_{WS-BrC}(\delta^{13}C) = C_1 \cdot \left(\frac{\delta^{13}C}{1000} + 1\right)^{C_2} \quad (35)$$

$$AAE(\delta^{13}C) = -C_3 \cdot \ln\left|\left(\frac{\delta^{13}C}{1000} + 1\right)\right| + C_4 \quad (36)$$

The aging model predicts a power-law dependence for the evolution of MAC_{WS-BrC} and AAE as a function of the $\delta^{13}C$ as per Eq.35 and Eq.36. The fit is shown in Fig. 4.

Note S4. Absorption measurements of $\text{MAC}_{\text{WS-BrC}}$ and AAE.

The mass-absorption cross section of WS-BrC at 365 nm ($\text{MAC}_{\text{WS-BrC } 365}$) is calculated in the manner as in (23, 26).

$$\text{MAC}_{\text{WS-BrC } 365} = \frac{b_{\text{abs}365}}{[\text{WSOC}]} = \frac{A_{\text{abs}365} - A_{\text{abs}700} \cdot \ln(10)}{[\text{WSOC}] \cdot L} \quad (37)$$

where b_{abs} is the absorption coefficient, WSOC is the water-soluble organic carbon concentration in solution, L is the light-path length (1 cm, for the currently used quartz cuvettes), and A_{abs} is the absorbance of the liquid extract (assuming that the scattering contribution to extinction is low) at 365 and 700 nm. To account for baseline drift during analysis A_{abs} at 700nm is used which is the average between 695 and 705 nm, where there is no absorption for ambient aerosol water extracts. $\ln(10)$ converts the relation between absorbance and transmittance from common logarithm (base 10) to the natural logarithm of gases.

The wavelength (λ) dependence of the WSOC absorption is calculated by fitting the absorption Ångström exponent (AAE) using the following relation:

$$\frac{A(\lambda_1)}{A(\lambda_2)} = \left(\frac{\lambda_2}{\lambda_1}\right)^{\text{AAE}} \quad (38)$$

The AAE was fitted within the range 330–400 nm to avoid interference from other light-absorbing solutes such as ammonium nitrate, sodium nitrate, and nitrate ions which absorb light at peaks near 308, 298, and 302 nm, respectively. There may also be an effect of pH on differences in absorptivity between molecular and anions but the effect is likely less for the majority of organic molecules.

Note S5. Estimating the imaginary part of the refractive index of WS-BrC.

The imaginary part (K) of the refractive index ($m = n + iK$) is derived using the method as in (17) with the following equation:

$$K = (\text{MAC}_{\text{WS-BrC}} \cdot \rho \cdot \lambda) / 4\pi \quad (39)$$

Where $\text{MAC}_{\text{WS-BrC}}$ is the mass-absorption cross section of WS-BrC ($\text{m}^2 \text{g}^{-1}$), ρ is the effective density, λ is the wavelength for the computed $\text{MAC}_{\text{WS-BrC}}$. For the present WS-BrC study, an effective density of 1.19 g cm^{-3} is assumed for BrC in the derivation. $\text{MAC}_{\text{WS-BrC}}$ values are computed for 365 nm. The K values computed for BrC are shown in fig. S4.

Note S6. Testing a putative effect of pH on WS-BrC optical properties over the South Asian region.

Model: pH was calculated using an initial ISORROPIA-II model run. ISORROPIA-II is a thermodynamic equilibrium model for the K^+ - Ca^{2+} - Mg^{2+} - NH_4^+ - Na^+ - SO_4^{2-} - NO_3^- - Cl^- - H_2O aerosol system, which computes the particle liquid water content in equilibrium with the ambient relative humidity and considers the nonidealities between all dissolved major ions in solution. In the calculations of pH here, the hydrogen ion activity is taken to unity. Further descriptions of this model can be found here:

http://nenes.eas.gatech.edu/ISORROPIA/index_old.html. The model predicts a slight acidification trend between Delhi (6.00 ± 0.10), BCOB (5.96 ± 0.08) and MCOH (5.67 ± 0.10) during SAPOEX-16.

Measurement: The pH of WSOC extracts was measured using a pH meter (Radiometer Copenhagen, PHM 93) which was calibrated with buffer solutions of pH 4.00 and pH 7.00. The calibration accuracy reported by the pH meter was 99.80%. A control standard (made of potassium phosphate: 3.39 g/l and disodium phosphate dibasic dihydrate: 4.43 g/l) of pH 6.90 was used for quality control and quality assurance purposes. The average relative standard deviation of triplicate analysis for the control standard was < 1%.

The ratio of anion equivalence (AE) to cation equivalence (CE) was used as an indicator of aerosol acidity for sample selection: the sample with the highest, the lowest and an intermediate $\Sigma AE / \Sigma CE$ was selected for each site. It should be noted that the total inorganic acidity (TIA = $(nss-SO_4^{2-} + NO_3^- / \Sigma \text{ water soluble inorganic ion conc.})$) which is also an indicator of aerosol acidity (36), varied only slightly on average between the source-to-receptor sites during SAPOEX-16: Delhi (0.62 ± 0.12), BCOB (0.69 ± 0.08) and MCOH (0.72 ± 0.06).

Overall for the SAPOEX-16 campaign, 9 samples (3 from each site) were re-extracted for WSOC and measured for pH (in triplicates) along with light-absorption parameters (MAC_{WS-BrC} ₃₆₅, AAE). The results for the pH study are reported in table S2.

It is clear from table S2 that 1. The pH for WSOC extracts at Delhi, BCOB and MCOH are in good agreement with the $\Sigma AE/\Sigma CE$ ratio; 2. A slight acidification trend in pH of WSOC-extracts is conspicuous in the order Delhi-to-BCOB-to-MCOH, but the difference is comparably low ($\Delta pH_{\max} = 0.61$); 3. The small variability in pH doesn't explain the large differences in $MAC_{WS-BrC\ 365}$ and $AAE_{330-400\ nm}$ between the source-to-receptor sites during SAPOEX-16.

To further test the dependence of WS-BrC light-absorption on pH, a titration experiment was conducted. By adding small amounts of NaOH (0.01M) to the sample (MCO-3) from MCOH with the lowest pH (5.57) to shift the pH to the highest pH recorded at BCOB (6.02) and then shift the pH to the highest pH recorded at Delhi (6.18) we find that the change in pH had insignificant effect on the light-absorbance of the WSOC-extract and thus it can be concluded that small pH-difference does not explain the large differences in mass-absorption cross section ($MAC_{WS-BrC\ 365}$) and absorption Ångström Exponent ($AAE_{330-400\ nm}$) between source-to-receptor sites during SAPOEX-16 (fig. S6).

This conclusion is consistent with the fact that the presence of fine-mode mineral dust in the IGP region contributes to similar degree of acid processing of aerosols in the IGP outflow to the Bay of Bengal as in the IGP sites (36), thus balancing the aerosol acidity in the South Asian outflow.

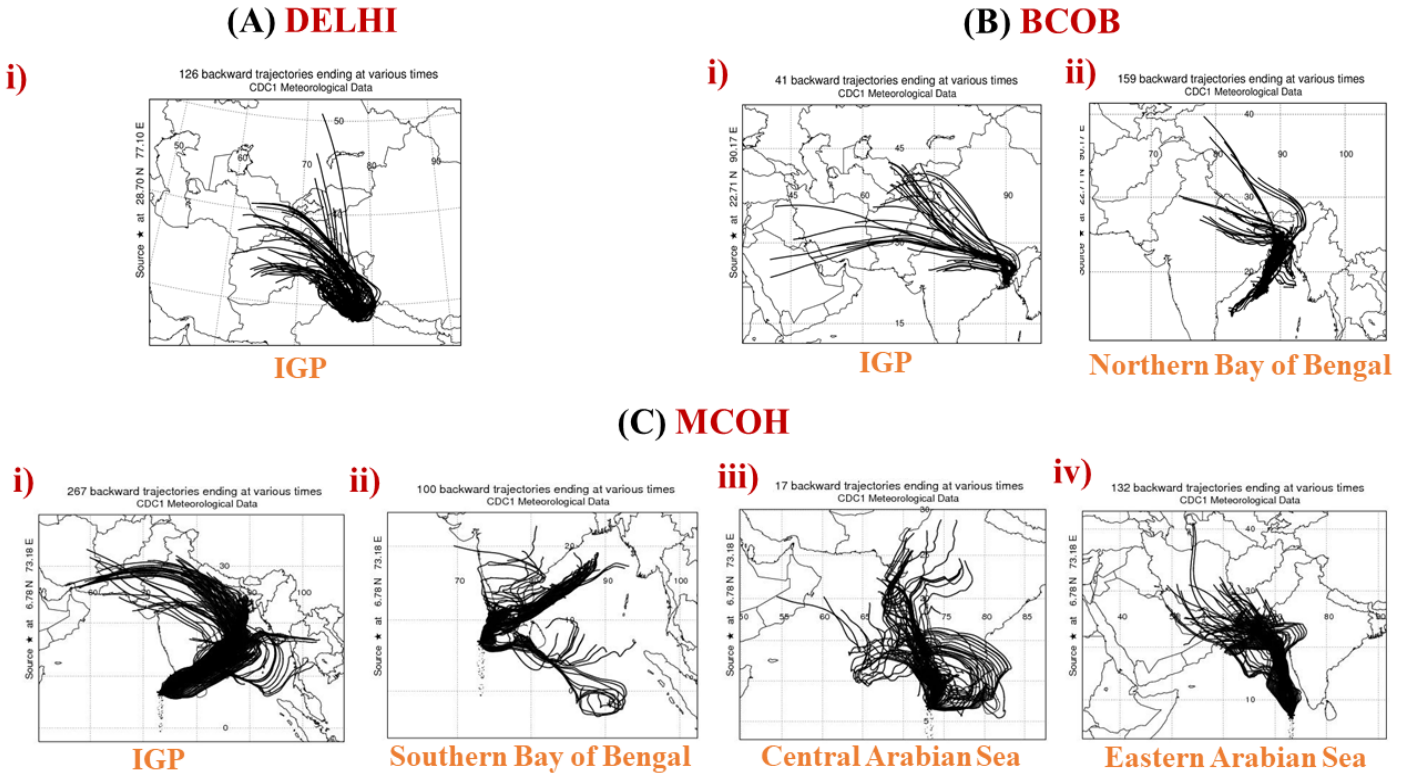


Fig. S1. Air mass clusters during SAPOEX-16. Nine-day air-mass back trajectories (BTs) were generated for Maldives Climate Observatory at Hanimaadhoo at an arrival height of 100 m, computed for every 3 h, using NOAA Hybrid Single-Particle Lagrangian Integrated Trajectory model (HYSPLIT), version 4. 5-day and 3-day BTs were also generated for Bangladesh Climate Observatory at Bhola (BCOB) and Delhi, respectively. The BTs were clustered as follows: **(A) Delhi** – i) Indo-Gangetic Plain (IGP). At **(B) BCOB** – i) IGP, ii) Northern Bay of Bengal (along with the eastern coast of India). At **(C) MCOH** – i) IGP, ii) Southern Bay of Bengal, iii) Central Arabian Sea (including southern India), iv) Eastern Arabian Sea (including western Indian margin).

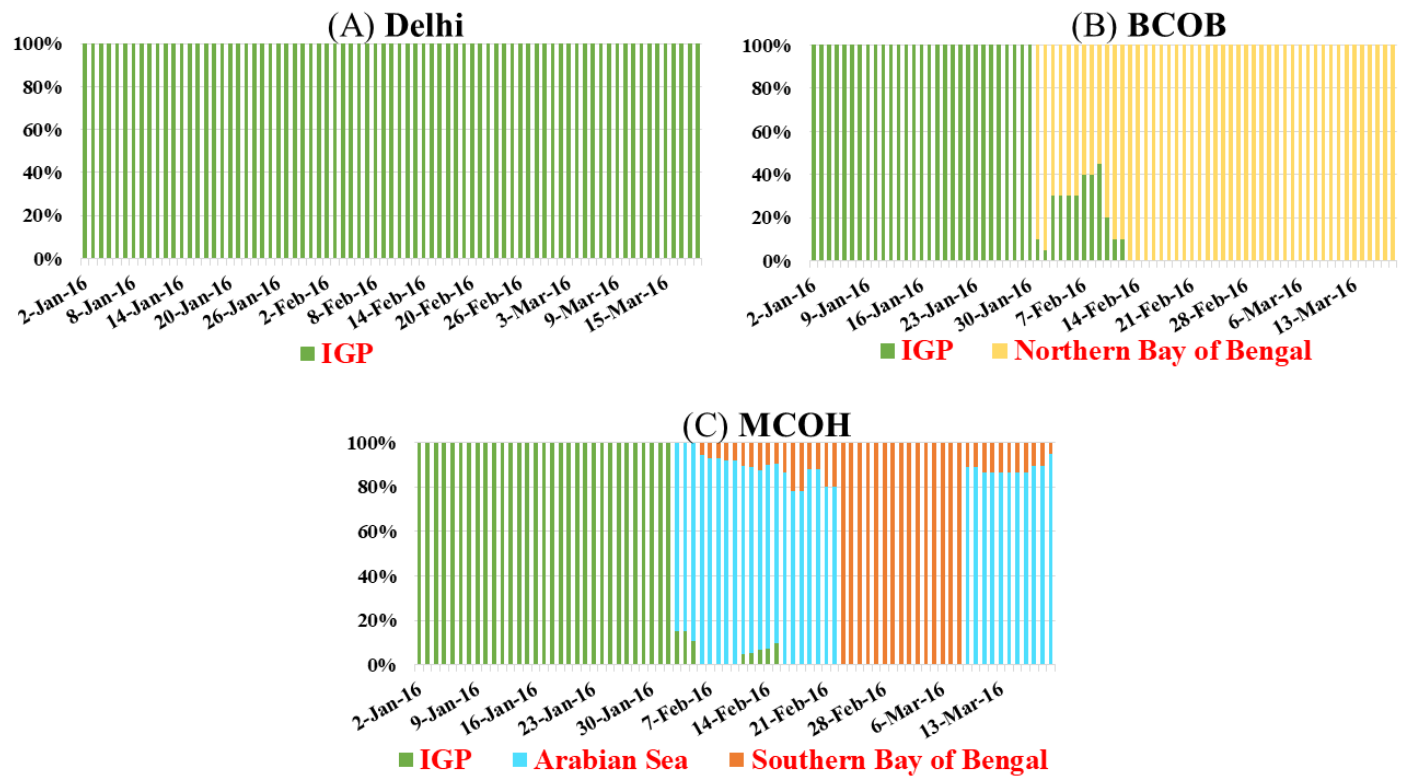


Fig. S2. Fractional contribution of air mass clusters during SAPOEX-16. For the sites **(A)** Delhi, **(B)** Bangladesh Climate Observatory at Bhola (BCOB) and **(C)** Maldives Climate Observatory at Hanimaadhoo (MCOH). Note the fractional contribution of Central and Eastern Arabian Sea is shown as a single air-mass cluster (Arabian Sea) at MCOH.

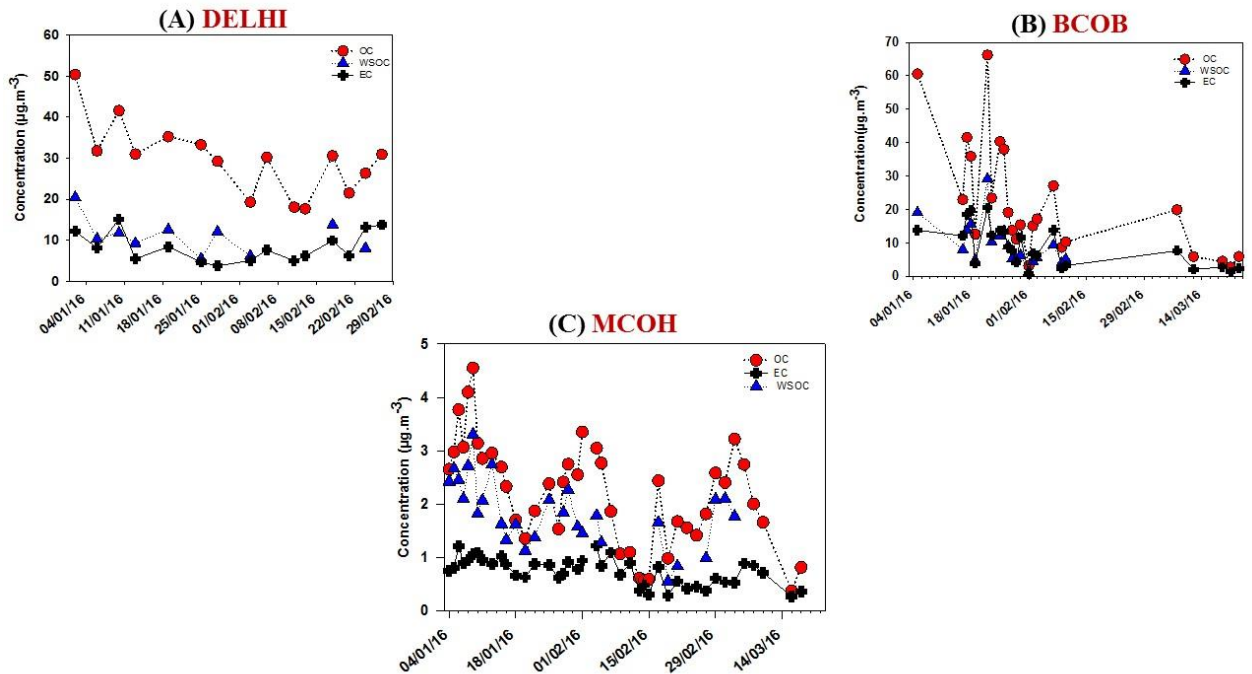


Fig. S3. Concentrations of EC, OC, and WSOC during SAPOEX-16. Concentrations of elemental carbon (EC), organic carbon (OC) and water-soluble organic carbon (WSOC) in aerosol fine fraction $\text{PM}_{2.5}$ at (A) Delhi, (B) Bangladesh Climate Observatory at Bholá (BCOB) and PM_1 at (C) Maldives Climate Observatory at Hanimaadhoo (MCOH). Note the order of magnitude difference in the concentrations between MCOH and BCOB, Delhi.

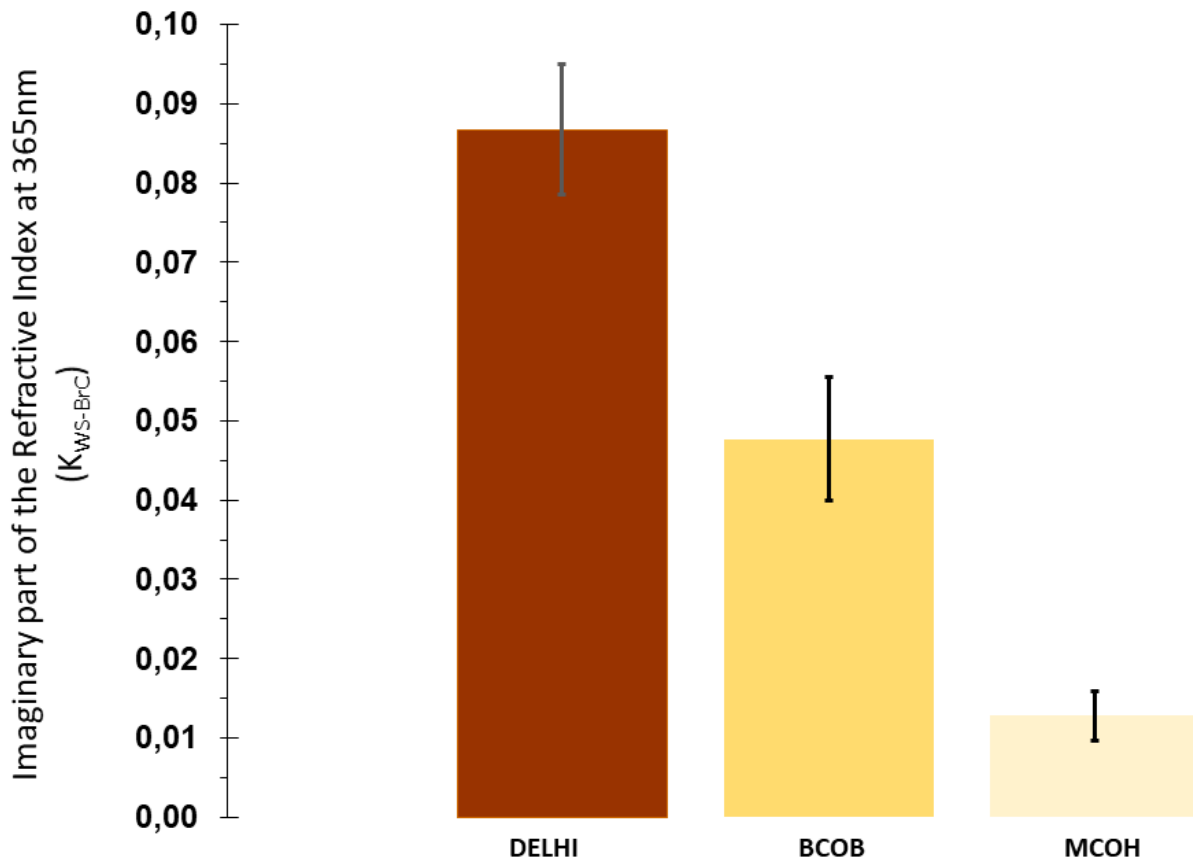


Fig. S4. Imaginary part of the refractive index (K_{WS-BrC}) at 365 nm. The imaginary part of the refractive index at 365nm is derived from the measured mass-absorption cross section of WS-BrC ($MAC_{WS-BrC\ 365}$) values based on Mie theory as explained in Note S5 and reported here as K_{WS-BrC} .

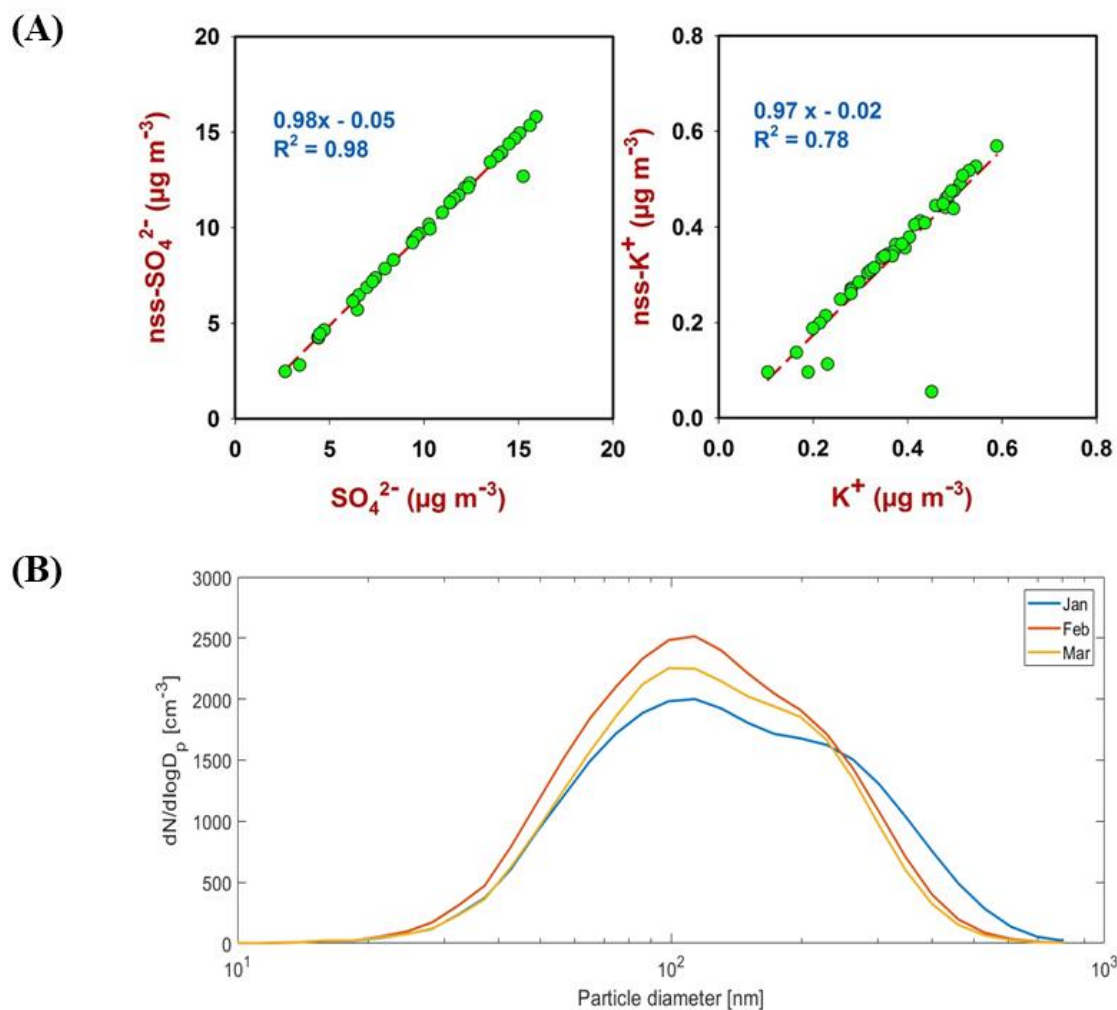


Fig. S5. Asserting the peripheral contribution of marine-biogenic sources at MCOH during SAPOEX-16. (A) Ratios of non-seasalt (nss)- SO_4^{2-} to total SO_4^{2-} and nss- K^+ to total K^+ , (B) Size-distribution of PM_{10} aerosols, at Maldives Climate Observatory at Hanimaadhoo (MCOH) during SAPOEX-16.

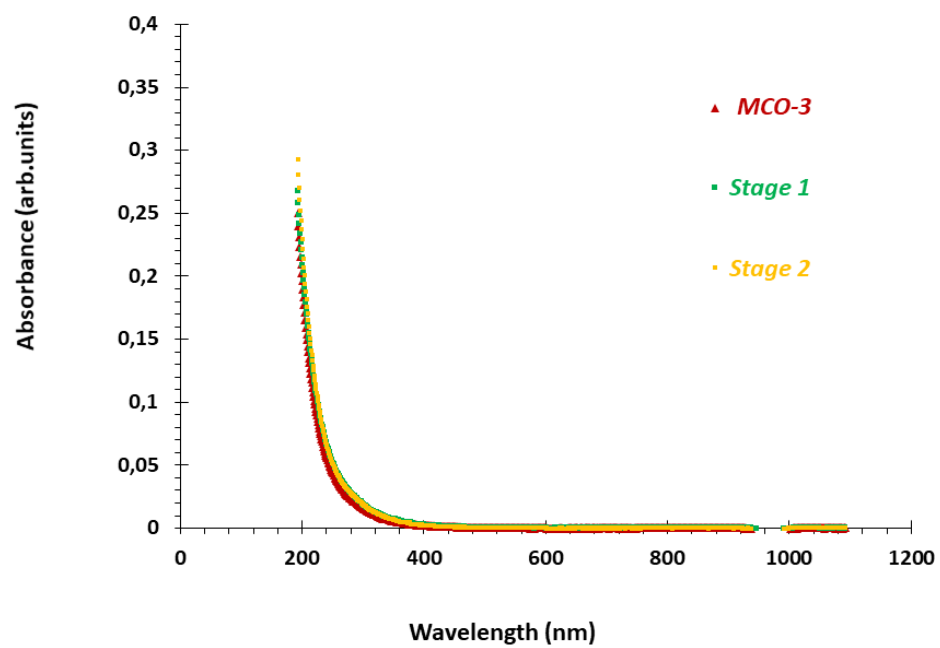


Fig. S6. Testing a putative effect of pH on WS-BrC optical properties over the South Asian region. Light-absorbance of the WSOC sample MCO-3 (pH=5.56) with increasing pH to Stage 1 (pH =6.02) and Stage 2 (pH =6.18); refer to table. S2 in ms Supp. Info. for pH data.

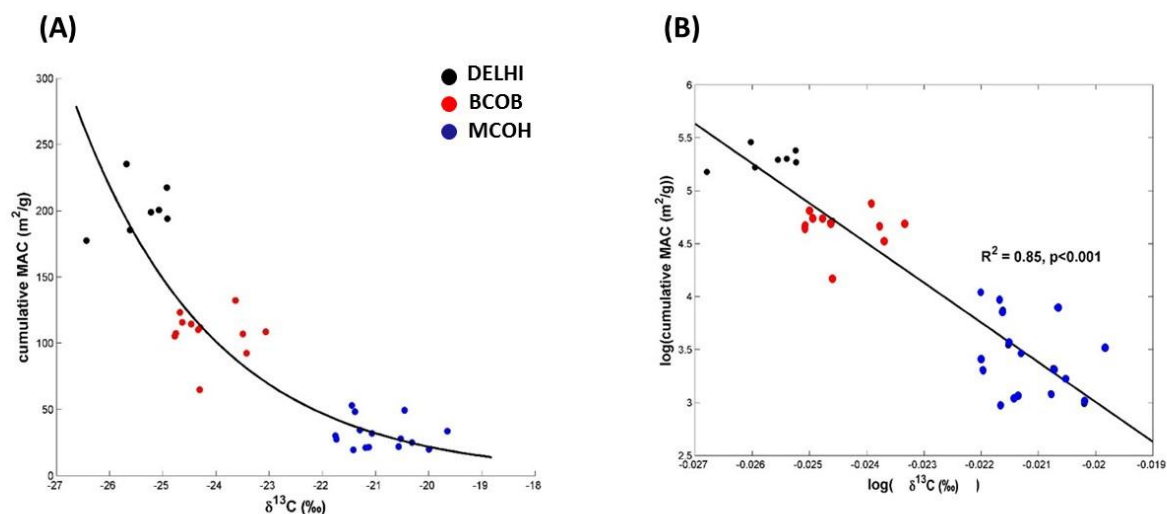


Fig. S7. Constraining the mixing of WSOC sources on WS-BrC light absorption in the South Asian outflow. (A) The dependence of cumulative (between 330 to 400 nm) mass-absorption cross section ($\text{MAC}_{\text{WS-BrC}}$) on $\delta^{13}\text{C}$ signature is non-linear (as opposed to the finding in Equation 7) implying that the $\delta^{13}\text{C}$ signature of water-soluble organic carbon (WSOC) is not driven by mixing of marine and terrestrial sources. **(B)** Logarithm of the parameters in A showing a better fit.

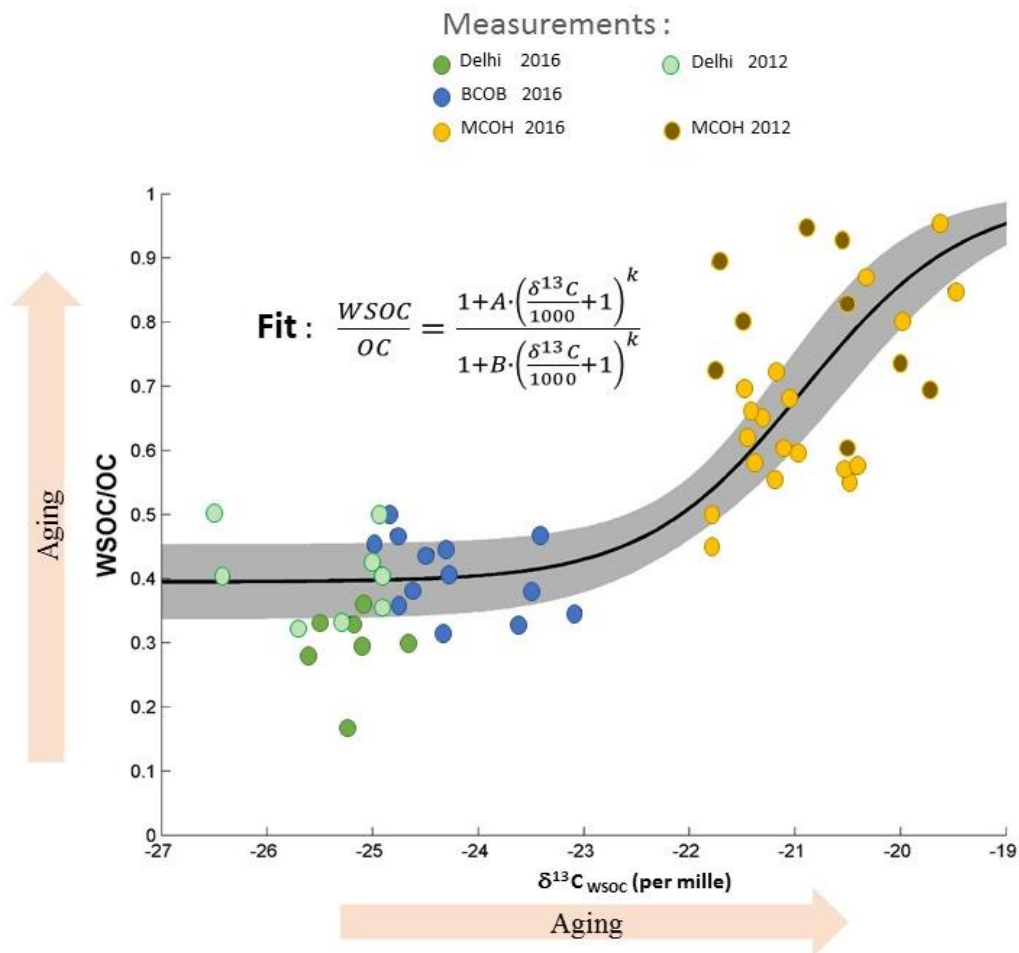


Fig. S8. Degradation of WSOC and WIOC during long-range transport in the South Asian outflow. The line in black represents the fit (Eq.15) and the shaded region represents two times the standard deviation. The enrichment of mass fraction of water-soluble organic carbon (WSOC) is possibly governed by the oxidative transformation of WSOC and transfer from the water-insoluble to water-soluble pool of organic carbon in the South Asian outflow. The ambient field data of Delhi, BCOB and MCOH during SAPOEX-16 as well as previous campaigns from (23, 26) performed separately at Delhi and MCOH are in good agreement with the empirical formulation of the kinetics and the fitting curve shown by the goodness of fit in terms of root-mean-square deviation RMSD: 0.34 and normalized root-mean-square deviation NMRSD: 0.27.

Table S1. Concentrations (mean \pm SD) and element mass ratios of carbonaceous species during SAPOEX-16.

Parameter	Delhi (n=15)	BCOB (n=24)	MCOH (n=43)
PM ($\mu\text{g}\cdot\text{m}^{-3}$)	208 \pm 57	103 \pm 70	26 \pm 10
OC ($\mu\text{g}\cdot\text{m}^{-3}$)	29 \pm 8	21 \pm 17	2 \pm 1
EC ($\mu\text{g}\cdot\text{m}^{-3}$)	8 \pm 3	8 \pm 6	0.7 \pm 0.2
OC/EC	4 \pm 3	3 \pm 1	2 \pm 1
nss-K ⁺ /EC	0.6 \pm 0.4	0.4 \pm 0.1	0.5 \pm 0.1
nss-SO ₄ ²⁻ /EC	2 \pm 2.0	3 \pm 3.0	14 \pm 3.0

Table S2. pH of aerosol WSOC extracts during SAPOEX-16. pH was measured in triplicates (n=3) for each sample.

Site	Sample ID	Σ AE/ Σ CE	Average pH, n=3 (Mean \pm Std.)	WSOC/OC (%)	AAE _{330-400nm}	MAC _{WS-BrC 365} (m ² g ⁻¹)
DELHI	DHL-1	0.73	6.18 \pm 0.027	31	4.00	2.49
	DHL-2	0.97	6.14 \pm 0.010	33	4.14	2.36
	DHL-3	1.18	6.11 \pm 0.005	36	4.44	2.24
BCOB	BCO-1	1.02	6.02 \pm 0.007	51	5.11	1.45
	BCO-2	1.18	5.69 \pm 0.012	42	5.54	1.35
	BCO-3	1.27	5.67 \pm 0.008	44	5.68	1.38
MCOH	MCO-1	0.93	6.03 \pm 0.019	86	6.63	0.52
	MCO-2	1.13	5.68 \pm 0.041	85	7.03	0.36
	MCO-3	1.27	5.57 \pm 0.006	91	7.13	0.31